Optics Letters

Optical phase conjugation in backward Raman amplification

QING JIA,[1,2] KENAN QU,[1] AND NATHANIEL J. FISCH[1]

[1]Department of Astrophysical Sciences, Princeton University, Princeton, New Jersey 08544, USA
[2]Currently at the School of Nuclear Science and Technology, University of Science and Technology of China, Hefei 230026, China

Received 12 May 2020; revised 28 July 2020; accepted 12 August 2020; posted 12 August 2020 (Doc. ID 397321); published 14 September 2020

Compression of an intense laser pulse using backward Raman amplification (BRA) in plasma, followed by vacuum focusing to a small spot size, can produce unprecedented ultrarelativistic laser intensities. The plasma density inhomogeneity during BRA, however, causes laser phase and amplitude distortions, limiting the pulse focusability. To solve the issue of distortion, we investigate the use of optical phase conjugation as the seed pulse for BRA. We show that the phase conjugated laser pulses can retain focusability in the nonlinear pump depletion regime of BRA, but not so easily in the linear amplification regime. This somewhat counterintuitive result is because the nonlinear pump depletion regime features a shorter amplification distance, and hence less phase distortion due to wave–wave interaction, than the linear amplification regime.

https://doi.org/10.1364/OL.397321

Generating strong laser pulses and delivering them precisely to certain target regions represent two major endeavors in laser technology development. They are important in many applications, such as laser-based particle accelerators, inertial confinement fusion, laser surgery, and laser-based weapons. Advances of these two aspects of laser technologies are often dependent on each other. Intense laser pulses induce strong refraction during propagation, which, on the other hand, limits the amplification of the laser pulses themselves. State-of-the-art laser intensities are currently obtained by splitting the pulse into multiple components for amplification before compressing/recombining them either in the frequency domain, such as chirped pulse amplification, or in the space domain. For the process of pulse compression/recombination [1], it was proposed to use backward Raman amplification (BRA) [2–5] in plasma rather than using solid-state optical components to avoid the thermal damage issue. BRA eliminates the major hurdle in ultrahigh peak power laser pulse compression, holding the promise, in principle, of exawatt to zettawatt pulses [1].

In plasma BRA, an active plasma wave mediates the laser energy transfer from a long pump pulse to a counterpropagating short seed pulse at a lower frequency. Because of its high growth rate, an initial weak seed laser pulse can gain an e-fold intensity increase in a few laser cycles in the linear amplification stage. The fast-growing seed pulse quickly depletes the pump pulse and captures the pump energy in the short seed pulse. In the nonlinear pump depletion stage, the seed pulse amplitude grows linearly with time while its duration decreases inversely with time. It is this nonlinear stage that provides the vital compression to the final ultrashort pulse. For 1 μm-wavelength radiation, ultrafast compression of BRA can theoretically achieve nearly relativistic intensities (10^{17} W/cm^2), which is five orders of magnitude higher than the output intensity of 10^{12} W/cm^2 from a typical chirped-pulse-amplification compressor.

The relativistic intensity limit in plasma can be overcome by transversely focusing the pulse to higher intensity, which is achieved outside the plasma. Thus, a properly shaped laser pulse, if remaining well focused during amplification, can deliver an unprecedented ultrarelativistic intensity at the focal point after exiting the plasma [3,4]. Two-dimensional numerical simulations find that the BRA is robust to a broad range of pump and seed perturbations in homogeneous plasmas [6]. Even a pump laser with finite coherence could be efficiently compressed into a short pulse in the nonlinear amplification stage [7]. In BRA experiments, one of the major restrictions is often related to ensuring the seed pulse quality when it interacts with the pump laser. A pre-focused seed pulse may deteriorate when propagating through random plasma inhomogeneities [8,9]. The reduction of seed peak intensity delays the onset of nonlinear pump depletion and costs in energy transfer efficiency. The scattering might also create precursors that cause unwanted premature pump depletion [10]. Unfortunately, the plasma density fluctuates randomly in space, and its effect is too complicated to somehow be mitigated by adjusting the laser phasing.

A phase conjugation (PC) wave can compensate for the phase distortion in the same random plasma by reversing the time–symmetry of pulse propagation [11–19]. Its implementation in seeding plasma Raman amplification could possibly avoid the vulnerability of pulse scattering by plasma density inhomogeneity. Consider the schematics in Fig. 1. Through an ionizable mirror, a focused laser pulse at frequency ω_b is sent into a random plasma and reflected by a PC mirror to create the seed pulse. The PC seed pulse then propagates against a pump pulse at frequency ω_a in the same plasma. Without seed–pump

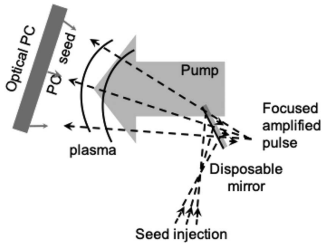

Fig. 1. Schematics of using optical phase conjugation of a pre-focused seed pulse in backward Raman amplification to counteract the distortion due to plasma density fluctuation.

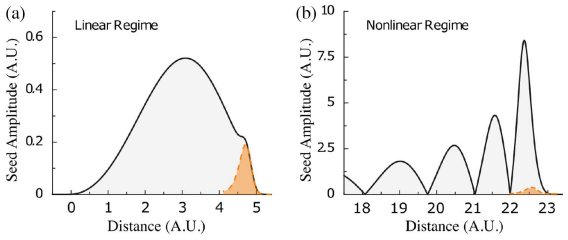

Fig. 2. Comparisons of the seed pulse (orange dashed curves) and the amplified pulse (black solid curves) in (a) the linear stage at $(|a|V)t = 4.5$ and (b) the nonlinear stage at $(|a|V)t = 22.5$ of BRA, respectively.

interaction, the seed pulse can focus at the original focal point despite plasma inhomogeneity. With a proper pump, the seed pulse gets amplified through the BRA process. The condition for perfect phase correction and pulse intensity restoration using PC is that the medium is stationary and lossless. While the plasma density dynamics could be negligible during the passage of the seed pulse, it is not known whether the amplification process changes the focusability of the PC seed pulse.

To analyze the evolution of the amplified seed, we denote the PC seed pulse as $\mathbf{E}_b = \mathbf{u}_b(\mathbf{r})e^{i\phi_b(\mathbf{r})}e^{-i(k_b x+\omega_b t)}$ with a complex amplitude $\mathbf{u}_b$ and a wavevector k_b. Here, $\phi_b(\mathbf{r})$ is a fluctuating phase that would gradually decrease and be perfectly compensated for at the plasma boundary. When the PC seed interacts with a counterpropagating pump pulse $\mathbf{E}_a = \mathbf{u}_a(\mathbf{r})e^{i\phi_a(\mathbf{r})}e^{i(k_a x-\omega_a t)}$, the ponderomotive potential of the pump–seed beating induces a plasma wave $\mathbf{E}_f = \mathbf{u}_f(\mathbf{r})e^{i\phi_f(\mathbf{r})}e^{i(k_f x-\omega_p t)}$ if the $\omega_a - \omega_b = \omega_p$. Here, $\mathbf{u}_{a,f}$, $k_{a,f}$, and $\phi_{a,f}(\mathbf{r})$ denote the complex amplitude, wavevector, and random phase of the pump laser/plasma wave, respectively. The BRA process can be described through the simplified coupled wave equations [3,4]

$$(\partial_t - c\partial_x)a = -Vbf, \quad (\partial_t + c\partial_x)b = Vaf^*, \quad \partial_t f = Vab^*, \tag{1}$$

where a and b $[= eu_{a,b}e^{i\phi_{a,b}(\mathbf{r})}/(m_e c^2\omega_{a,b})]$ denote the complex envelopes of the pump and seed pulses, respectively, $f = eu_f e^{i\phi_f(\mathbf{r})}/(2m_e c\omega_p)$ denotes the complex envelope of the plasma wave, $V \approx \sqrt{\omega_a\omega_p}/2$ is the three-wave interaction rate, e is the natural charge, m_e is the mass of an electron, and c is the speed of light. Note that Eq. (1) does not include transverse Laplacian terms because we neglect the change of interaction rate due to a small transverse phase mismatch. We assume that the transverse phase of the new wave at the time of generation is determined solely by the existing waves.

During BRA, the generated plasma wave further interacts with the pump and causes energy transfer to the seed pulse. The seed amplitude $|\mathbf{u}_b(\mathbf{r})|$ is certainly changed during BRA. But what governs the pulse focusability is the dynamics of the laser phase $\phi_b(\mathbf{r})$. For convenience, we separately describe the seed pulse and the amplified pulse (the so-called probe pulse) as b_0 and b_1, respectively, although they have the same frequency and wavevector, i.e., $b = b_0 + b_1$. Since the plasma wave f is created by the combination of laser pulses a and b, it has the conjugate phase of the seed, $f \sim b_0^*$. The amplified pulse b_1, when propagating through the plasma wave, integrates over the plasma waves with all phases. In the early stage of amplification without pump depletion ($|a| \equiv$ Const.), the amplified pulse can be solved exactly [20] without explicitly including f:

$$b_1(t, x) = \int_0^x G(t, x - x')b_0(x')\mathrm{d}x', \tag{2}$$

$$G(t, x) = \sqrt{\frac{|a|^2V^2}{c^2}\frac{x}{ct - x}}\, I_1\left(\sqrt{\frac{2|a|^2V^2}{c^2}x(ct - x)}\right), \tag{3}$$

where I_1 is the first-order modified Bessel function. For illustration, we show in Fig. 2(a) the comparison of the seed pulses before and $t = 4.5(|a|V)$ after amplification. Equation (2) shows that the amplified seed pulse envelope is the convolution of Green's function G and the original seed pulse b_0, which has a random phase $e^{i\phi_b(\mathbf{r},x)}$. Since G maximizes at $x = ct/2$, the convolution operation mixes all the seed phases, and the resulting amplified pulse has different phases. Hence, the amplified pulse b_1 at its peak does not retain the focusability of the PC seed in the linear stage of BRA.

The amplification process becomes different in the nonlinear pump depletion stage, which happens when the seed becomes sufficiently strong. In this stage, the strong seed quickly depletes the pump within a short interaction distance. The analytical form of the Green's function becomes cumbersome, but pictorially, its peak shifts from $x = ct/2$ to $x \sim ct$. As illustrated in Fig. 2(b), the amplified pulse gains preferentially more pump energy only if it closely follows the seed pulse. The shadowing effects of the rear layer amplification due to pump depletion, controversially, benefit the pulse focusability by eliminating the unwanted convolution process. In the nonlinear regime, the transverse phase front is carried over from the PC seed pulse to the plasma wave and then immediately to the amplified pulse. The local phase of $b_1(x)$ at the leading pulse spike closely resembles the phase $\phi_b(\mathbf{r})$. Hence, the focusability of the PC seed remains in the nonlinear regime. Importantly, the pump phase fluctuation due to the plasma inhomogeneity does not affect the focusability because only the pump intensity $|a|^2$ appears in the interaction, as seen in Eqs. (2) and (3).

Preparing an intense seed for reaching the nonlinear stage of BRA requires tight focusing of the laser pulse. Such a seed pulse contains a broad spectrum of wavenumbers, and each wavenumber component, after propagation in an inhomogeneous plasma, could accumulate a different phase $\phi_b(\mathbf{k}, \mathbf{r})$, i.e., $\mathbf{E}_b = \frac{1}{\sqrt{2\pi}}\int \mathbf{u}_b(\mathbf{k}, \mathbf{r})e^{i\phi_b(\mathbf{k},\mathbf{r})}e^{-i(\mathbf{k}_b\cdot\mathbf{r}+\omega_b t)}\mathrm{d}^3k_b$. In the regions where different wavenumber components have similar phases, they constructively interfere and create local amplitude peaks; otherwise, they destructively interfere and create local

amplitude troughs. The local intensity peaks feature higher seed intensities with shorter spike duration similar to those in a multifrequency Raman amplifier [21]. Since the nonlinear growth rate depends on the seed intensity, the onset of local peaks benefits rapidly reaching the nonlinear stage of amplification.

The fluid model Eq. (1) assumes quasi-frequency matching and phase matching. The matching conditions, in principle, do not hold in an inhomogeneous plasma due to fluctuation of the local plasma frequency and scattering of the laser pulses. The fluctuation of plasma frequency could be compensated for by the broad spectra of the local intensity peaks. The mismatch of the pulse wavefronts can, to a certain degree, also be mitigated with a PC seed pulse: since the propagation of the PC seed pulse is a time reversal of a counterpropagating focused pulse, the wavefront of the PC seed pulse at any certain location is similar to that of the counterpropagating pump pulse when neglecting their frequency detuning and different Rayleigh lengths. However, these analyses must be checked more rigorously. In the following, we show kinetic particle-in-cell (PIC) simulations to demonstrate the advantage of PC seeds compared to other types of seeds in BRA.

The PIC simulations are conducted in two dimensions (x and y) using the full-relativistic kinetic code EPOCH [22]. For reference, we first demonstrate BRA of a tightly focused laser seed in a homogeneous plasma. As illustrated in Fig. 3(a), a pump pulse propagating in the x direction interacts with a counterpropagating seed pulse in a 0.53 mm long plasma. The pump pulse has a wavelength $\lambda_{\text{pump}} = 0.8\ \mu\text{m}$ and intensity $I_{\text{pump}} = 1.2 \times 10^{16}\ \text{W/cm}^2$. The Gaussian-shaped seed pulse has a wavelength $\lambda_0 = 0.889\ \mu\text{m}$ and, after exiting the plasma, is focused at $X = 0$ with a waist $w_0 = 8\lambda_0$. The electron number density of the homogeneous plasma is $n_0 = 0.01 n_c$, where $n_c = 1.74 \times 10^{27}\ \text{m}^{-3}$ is the critical density for the pump pulse. The size of the simulation box is $1000\lambda_0 \times 128\lambda_0$ with 10 cells per λ_0 in both x and y directions. Periodic boundary conditions are applied in the y direction, and 64 electrons per cell are placed between $X = 200\lambda_0$ and $X = 800\lambda_0$. The seed intensity profiles at different propagation distances are shown in Figs. 3(d), 3(c), and 3(b). The parameters are chosen such that Raman scattering dominates over unwanted parasitic instabilities, and the final pulse, as shown in Fig. 3(b), exhibits a smooth and regular tightly focused profile.

If the same pre-focused seed pulse is sent into an inhomogeneous plasma for amplification, the seed pulse becomes scattered and loses focusability after exiting the plasma. According to Ref. [8], the scale length of a laser pulse losing energy due to scattering is

$$l_s = 4\omega_b^2 c^2/(\omega_p^4 \langle \tilde{n}^2 \rangle^{1/2} l), \tag{4}$$

where $\tilde{n}$ is the relative density fluctuation, and l is the correlation length defined by $\langle \tilde{n}(\vec{r})\tilde{n}(\vec{r}+\vec{R})\rangle/\langle \tilde{n}^2\rangle = \exp[-\pi(X^2+Y^2)/l^2]$. For efficient BRA, the correlation length needs to be longer than the plasma wavelength $\lambda_e = 2\pi c/\omega_p = 9\lambda_0$. We thus choose $l = 40\lambda_0$ and $\tilde{n}/n_0 = 0.17$. The simulation results show that the initially high-quality laser pulse [Fig. 3(g)] has completely lost its focusability at the exit [Fig. 3(f)]. The pulse profile at the focal plane [Fig. 3(e)] is separated into more than seven visible speckles, and the peak intensity $1.3 \times 10^{17}\ \text{W/cm}^2$ is only a fraction of the focused pulse shown in Fig. 3(b). The pulse energy in the central region reveals the reduced energy transfer efficiency.

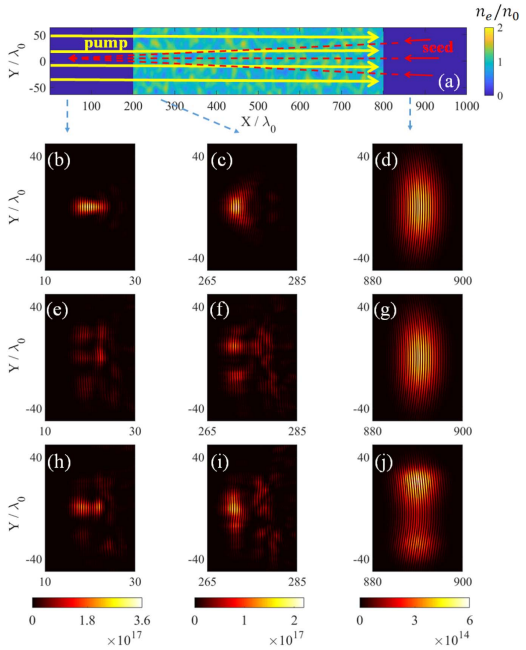

Fig. 3. (a) Schematics of the PIC simulations; color mapping shows the inhomogeneous plasma density. (d)–(b) Three snapshots of the intensity profiles of a pre-focused seed pulse during BRA in homogeneous plasma. (g)–(e) Pre-focused seed pulse in inhomogeneous plasma. (j)–(h) PC seed pulse in inhomogeneous plasma. The arrows below (a) illustrate the position of the snapshots.

We next replace the pre-focused seed pulse with a PC seed pulse and verify its performance of BRA in inhomogeneous plasma. The PC seed pulse, shown in Fig. 3(j), is obtained by sending a tightly focused pulse from $X = 0$ through the inhomogeneous plasma and extracting the amplitude and phase information of the pulse when it reaches $X = 900\lambda_0$. We then numerically take its PC and send it back to the plasma for BRA. Although the PC seed pulse exhibits a disrupted intensity profile at $X = 900\lambda_0$, it gradually recovers its focusability when propagating through the same inhomogeneous plasma. When it approaches the plasma boundary at $X = 200\lambda_0$, its intensity profile shows a regular focusing wavefront followed by several darker speckles, as shown in Fig. 3(i). The peak intensity of the main pulse is similar to that in Fig. 3(c). The darker speckles that are separated from the leading pulse are the results of linear amplification, and hence they do not retain the PC wavefront. After propagating in vacuum, the amplified pulse at $X = 0$ is able to focus into the short pulse [Fig. 3(h)] together with a dark halo. The peak intensity reaches $2.5 \times 10^{17}\ \text{W/cm}^2$, which is almost twice larger than the amplified pulse using a pre-focused seed in the same inhomogeneous plasma.

Further increasing the energy transfer efficiency and eliminating the unfocused speckles could be achieved by reducing the length of the linear amplification stage, e.g., with stronger seed pulses. A criterion for reaching the advanced nonlinear stage is that the seed intensity exceeds the pump intensity. For verification, we change the initial seed intensity from below the pump intensity ($2.5 \times 10^{14}\ \text{W/cm}^2$) to several times above that and repeat the PIC simulations sketched in Fig. 3(a). The results shown in Fig. 4 compare the peak intensity and the pulse energy

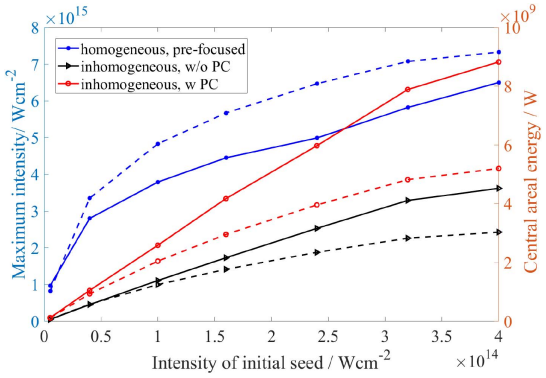

Fig. 4. Peak intensity (left axis, solid curves) and pulse energy (right axis, dashed curves) of the amplified seed at the focal plane with varying initial seed intensities. The three groups of curves are the results of using pre-focused seed in homogeneous plasma (blue dots), pre-focused seed in inhomogeneous plasma (black triangles), and PC seed in inhomogeneous plasma (red circles).

of the final focused amplified pulse. At very low seed intensity, BRA works mostly in the linear regime, and the amplified pulse does not retain the wavefront of the seed pulse. As expected, the PC seed pulse performs similarly to a pre-focused pulse. With higher initial seed intensities, the length of linear amplification decreases and the length of nonlinear amplification increases. In Fig. 4, we find that the amplified pulse intensity of a PC seed grows quicker than that of a pre-focused pulse. It approaches the pulse intensity from a homogeneous plasma when $I_{seed} \sim I_{pump}$. More interestingly, the simulation results in the region $I_{seed} > I_{pump}$ demonstrate that a PC seed pulse could be amplified to a pulse with higher intensity than a pre-focused pulse despite the plasma inhomogeneity. We also compare the amplified pulse energy in the $(8\lambda_0)^2$ region for different BRA schemes. The results in Fig. 4 yield the same conclusion that PC seed pulses can gain more energy than pre-focused pulses in the nonlinear amplification regime, although they cannot restore as much energy as the ideal case of homogeneous plasma.

The 2D PIC simulations clearly demonstrate the capability of retaining focusability of a strong PC seed pulse in BRA. Note that, should the PC pulse propagate with complete fidelity, it could in principle harm the seed laser; this can be avoided by using a disposable mirror to reflect the low-intensity seed pulse from the seed laser into the plasma, as illustrated in Fig. 1. The very high-intensity counterpropagating amplified pulse would then obliterate the mirror rather than harm the laser source. Since the wavefront of the amplified pulse resembles that of the initial seed pulse, the pulse can be focused even behind an aberrating medium. This scheme may have advantages in applications such as laser fusion and high-power radiation transmission where optical aberrations due to plasma/air density fluctuation impedes the focusing of laser power.

The full potential of this method can be realized only by first creating strong PC seed pulses. The time for seed creation and round-trip propagation cannot exceed the time scale of the aberration dynamics. For plasmas, the relevant time scale is determined by ion motion, which is in the ns scale for plasmas of interested density. The methods with stimulated Brillouin scattering [23] and degenerated four-wave mixing [11] in crystal are too slow and cannot resist high pulse intensities. A potentially viable method for PC is using stimulated emission [18,19,24,25]: an amplifying medium with population inversion is placed in a scattering medium, and the PC backscattered light is amplified when propagating. The lasing process contributes both to increasing the output pulse energy and to reducing the formation time of PC. The reported experiments have demonstrated PC of a 160 fs pulse at the μJ energy level. An upgrade of such a setup might reach both the required time scale and pulse intensity.

Funding. Air Force Office of Scientific Research (FA9550-15-1-0391); National Nuclear Security Administration (DE-NA0002948, DE-NA0003871).

Disclosures. The authors declare no conflicts of interest.

REFERENCES

1. G. Mourou, N. Fisch, V. Malkin, Z. Toroker, E. Khazanov, A. Sergeev, T. Tajima, and B. L. Garrec, Opt. Commun. **285**, 720 (2012).
2. G. Shvets, N. J. Fisch, A. Pukhov, and J. Meyer-ter Vehn, Phys. Rev. Lett. **81**, 4879 (1998).
3. V. M. Malkin, G. Shvets, and N. J. Fisch, Phys. Rev. Lett. **82**, 4448 (1999).
4. V. M. Malkin, G. Shvets, and N. J. Fisch, Phys. Plasmas **7**, 2232 (2000).
5. V. M. Malkin, G. Shvets, and N. J. Fisch, Phys. Rev. Lett. **84**, 1208 (2000).
6. G. M. Fraiman, N. A. Yampolsky, V. M. Malkin, and N. J. Fisch, Phys. Plasmas **9**, 3617 (2002).
7. M. R. Edwards, K. Qu, J. M. Mikhailova, and N. J. Fisch, Phys. Plasmas **24**, 103110 (2017).
8. A. A. Solodov, V. M. Malkin, and N. J. Fisch, Phys. Plasmas **10**, 2540 (2003).
9. J. P. Palastro, D. Gordon, B. Hafizi, L. A. Johnson, J. Peñano, R. F. Hubbard, M. Helle, and D. Kaganovich, Phys. Plasmas **22**, 123101 (2015).
10. Y. A. Tsidulko, V. M. Malkin, and N. J. Fisch, Phys. Rev. Lett. **88**, 235004 (2002).
11. R. W. Hellwarth, J. Opt. Soc. Am. **67**, 1 (1977).
12. A. Yariv and D. M. Pepper, Opt. Lett. **1**, 16 (1977).
13. D. G. Steel and J. F. Lam, Opt. Lett. **4**, 363 (1979).
14. A. A. Andreev, A. A. Betin, V. Mitropol'skii, and A. N. Shatsev, Zh. Eksp. Teor. Fiz **92**, 1636 (1987).
15. Y. Kitagawa, R. L. Savage, and C. Joshi, Phys. Rev. Lett. **62**, 151 (1989).
16. J. F. Federici, IEEE Trans. Plasma Sci. **19**, 549 (1991).
17. C. Joshi, Y. Kitagawa, and A. Lal, J. Nonlinear Opt. Phys. Mater. **01**, 1 (1992).
18. K.-H. Lee, C.-H. Pai, M.-W. Lin, L.-C. Ha, J.-Y. Lin, J. Wang, and S.-Y. Chen, Phys. Rev. E **75**, 036403 (2007).
19. Y. J. Ding, Opt. Lett. **37**, 4792 (2012).
20. K. Qu, I. Barth, and N. J. Fisch, Phys. Rev. Lett. **118**, 164801 (2017).
21. I. Barth and N. J. Fisch, Phys. Rev. E **97**, 033201 (2018).
22. T. D. Arber, K. Bennett, C. S. Brady, A. Lawrence-Douglas, M. G. Ramsay, N. J. Sircombe, P. Gillies, R. G. Evans, H. Schmitz, A. R. Bell, and C. P. Ridgers, Plasma Phys. Controlled. Fusion **57**, 113001 (2015).
23. B. Y. Zel'Dovich, V. I. Popovichev, V. V. Ragul'Skii, and F. S. Faizullov, Sov. J. Exp. Theor. Phys. Lett. **15**, 109 (1972).
24. G. S. He, Y. Cui, M. Yoshida, and P. N. Prasad, Opt. Lett. **22**, 10 (1997).
25. G. S. He, H.-Y. Qin, Q. Zheng, P. N. Prasad, S. Jockusch, N. J. Turro, M. Halim, D. Sames, H. Ågren, and S. He, Phys. Rev. A **77**, 013824 (2008).